Breathing Behaviors in Common Marmoset (*Callithrix jacchus*)

Mitchell Bishop, Ariana Z. Turk, and [CA]Shahriar SheikhBahaei

Running title: Breathing Behaviors in Common Marmoset

Neuron-Glia Signaling and Circuits Unit, National Institute of Neurological Disorders and Stroke (NINDS), National Institutes of Health (NIH), Bethesda, 20892 MD, USA

Keywords: apnea, breathing behavior, common marmoset, *Callithrix jacchus*, hypoxia, hypercapnia, sigh, sniffing

[CA]Corresponding author:
Shahriar SheikhBahaei, PhD; Neuron-Glia Signaling and Circuits Unit, National Institute of Neurological Disorders and Stroke, National Institutes of Health, Bethesda, MD 20892, USA. Tel: +1 (301) 496-0956; Email: SheikhbahaeiS@ninds.nih.gov

Conflict of interest: The authors declare no competing financial interests.

Acknowledgements: This work was supported by the Intramural Research Program (IRP) of the NIH, NINDS and in part, by the IRP of NIMH. We are grateful for invaluable supports and discussions from Drs. David Leopold, Yogita Chudasama, and Jeffrey Smith. We also thank Dr. Gregory Funk for valuable consultations.

Abstract:

The respiratory system maintains homeostatic levels of oxygen (O_2) and carbon dioxide (CO_2) in the body through rapid and efficient regulation of frequency and dept (tidal volume) of breathing. The use of common marmoset (*Callithrix jacchus*), a New World non-human primate (NHP) model, in neuroscience is increasing, however, the data on their breathing is limited and their respiratory behaviors have yet to be characterized. Using Whole-body Plethysmography in room air as well as in hypoxic (low O_2) and hypercapnic (high CO_2) conditions, we sought to define breathing behaviors in an awake, freely behaving marmosets. Additionally, we instituted and optimized an analysis toolkit for unsupervised analysis of the respiratory activities in common marmoset. Our findings indicate that marmoset's exposure to hypoxia decreased metabolic rate and increased sigh rate. However, the hypoxic condition did not augment the ventilatory response as reported in other animals. Hypercapnia, on the other hand, increased both the frequency and tidal volume as expected. In this study, we shed light on the breathing behaviors of common marmosets in a variety of O_2 and CO_2 conditions to further understand the breathing behaviors in NHPs.

Introduction

Mammals rely on fresh and continuous supply of oxygen (O_2) from the environment and efficient removal of carbon dioxide (CO_2) and other metabolic waste products from their body. The intricate respiratory system ensures the homeostatic state of the arterial partial pressure of O_2 (PO_2) and CO_2 (PCO_2) in the blood by executing rhythmic movement of the respiratory pump, which include the intercostals and the diaphragm muscles. The inception of this rhythm occurs within the preBötzinger complex (preBötC), a functionally specialized region in the ventrolateral medulla of the brainstem (1,2). Activities of the preBötC are modulated by specialized peripheral and central chemosensors that adjust the respiratory drive for homeostatic level of PO_2 and PCO_2 (3–9).

A large number of studies on homeostatic control of breathing have been done on rodent models, in which the experiments are mostly performed during the day i.e., rodent's normal inactive period. Since, in general, rodents have relatively reduced chemosensitivities compared with primates (10), there is little assurance on if these results can effectively be extrapolated to humans. Therefore, use of non-human primates (NHPs) has been proposed to fill this gap and translate rodent data to humans (11). The common marmoset (*Callithrix jacchus*) is a New World NHP with a small body size similar to a rat (250 – 600 g). Ease of handling, high reproductive efficacy, and lack of zoonotic risks compared to Old World NHPs make marmoset an attractive and powerful NHP model for biomedical and neuroscience research (12).

Here, we used Whole-body Plethysmography to record breathing behaviors of awake common marmosets in room air, as well as during hypoxic (low inspired O_2) and hypercapnic (high inspired CO_2) conditions. We also helped developing an optimized analysis toolkit for unsupervised characterization of respiratory indices in laboratory animals. We found that exposure of marmosets to hypoxia decreased metabolic rate and increased sigh rate, while the hypoxic-induced augmentation of ventilatory response was diminished. On the other hand, hypercapnic conditions increased both frequency and depth of breathing similar to other mammals of similar size.

Material and Methods

Animals

We used seven adult common marmosets (*Callithrix jacchus*) for measurement of breathing behavior (3 males, 4 females; 378 ± 12 g). All experiments were performed in accordance with National Institutes of Health Guide for the Care and Use of Laboratory Animals. Animals were housed in temperature-controlled facilities on a normal light-dark cycle (12h:12h, lights on at 7:00 AM). They lived in paired or family-grouped housing and were given tap water *ad libitum*.

Measurement of marmoset respiratory activity

Marmoset respiratory activity was measured using a Whole-body Plethysmography. Awake animals were placed in the Plexiglas chamber (~3 L) which was flushed with 21% O_2, 79% N_2, 22-24 °C, at a rate of 1.2 L/min during measurements of baseline respiratory behavior (Figure 1). Concentrations of O_2 and CO_2 in the chamber were monitored using a fast-response O_2/CO_2 analyzer (ML206, AD Instruments). All experiments were performed at the same time of day (between 1000 and 1400 hours) to account for circadian changes in base level physiology (13).

For measuring the respiratory behaviors during hypoxia, following a 40-minute baseline period, the chamber was flushed with 10% O_2, 90% N_2, 22-24 °C, at a rate of 1.2 l min^{-1}. After 10 minutes of exposure to hypoxic conditions, the chamber was then flushed with the room air for another 30 minutes (Figure 2).

Marmoset respiratory activity was also measured during exposure to hypercapnic conditions. Following a 40-minute baseline period, the chamber was flushed with 6% CO_2, 60% O_2, 34% N_2, 22-24 °C, at a rate of 1.2 l min^{-1}. After 10 minutes of exposure to hypercapnic conditions, the chamber was then flushed with room air for another 30 minutes.

All respiratory data were acquired with Power1401 (CED; RRID:SCR_017282) interface and transferred to Spike2 software (CED; RRID: SCR_000903).

Calculation of metabolic rate

For measuring metabolic rate (MR), we calculated CO_2 production using the following equation

$$MR = \Delta CO_2 \text{ x flow rate } / \text{ body mass}$$

where ΔCO_2 is the percent change in the [CO_2], flow rate is the flow rate through the plethysmography chamber (1.2 l min^{-1}), and body mass is marmoset body mass (g).

Data analysis

Data were tested with Shapiro-Wilk test for normality and statistically compared in Prism 8 (Graphpad, Inc; RRID: SCR_002798). Plethysmography data were imported to Python using Neo Python package (14,15). We wrote a custom Python script using methods from Neurokit2, NumPy, and Pandas software packages (16–18). Neurokit2 methods were used for signal cleaning and extraction of instantaneous frequency, T_{TOT} (total time of breath), and amplitude (i.e., tidal volume) from trough to peak of the signals (Figure 3).

During hypoxia and hypercapnia challenges, we analyzed the respiratory signals in 1-minute epochs to consider local changes in respiration parameters.

Frequencies above 200 cycles per minute (~3.3 Hz) and amplitude above .5 a. u. were excluded from analysis, as they were likely artifact resulting from movement inside the chamber. The calculated V_T (tidal volume) was normalized to the body mass of each animal. High frequency breathing behavior (i.e., sniffing) was defined as any breathing frequencies above 150 cycles per minute (2.5 Hz). Apneas were defined by breathing cycles with T_{TOT} greater than 3 seconds. Augmented breaths (i.e., sighs) were readily identifiable by using the criteria described in rats (6) and measured during the baseline and experimental conditions.

Two measures of rate variability were also calculated as described elsewhere (19). SD1 is a measure of dispersion of T_{TOT} perpendicular to the line of identity in the Poincaré plots, therefore demonstrating short term variability. SD2 is a measure of dispersion of T_{TOT} along the line of identity in the Poincaré plots, demonstrating long term variability in respiratory rate.

Data Availability

All the data and codes will be available on the NGSC GitHub.

Results

Validation of the Neurokit2 as an analysis toolkit in experimental animal models

To analyze resting rate of breathing (f_R), tidal volume (V_T), and minute ventilation (V_E), we first benchmarked the Neurokit2 analysis toolkit against the conventional method of analyzing respiratory data (6,9) in conscious mammals. We did not identify any differences in values of f_R, V_T, and V_E.

Resting respiratory behavior in adult marmosets.

The f_R at room air (normoxia/normocapnia) calculated from breath-to-breath time (T_{TOT}) was similar in female (63 ± 12 breaths min^{-1}) and male (73 ± 15 breaths min^{-1}) adult marmosets (Figure 4). The V_T, calculated from trough to peak amplitude and normalized to body mass, was similar in female (3.5 ± 1.2 a. u.) and male (4.2 ± 1.1 a. u.) adult marmosets. Additionally, V_E was similar in female (2.9 ± 1.4 a. u.) and male (2.5 ± .7 a.u.) marmosets. Two marmosets (1 male and 1 female) showed prolonged breath holdings (11 ± 2 breaths hr^{-1} for 4.3 ± .1 min).

Hypoxic Ventilatory Response

We measured changes of f_R, V_T, and V_E during systemic hypoxic challenges (10% O_2 in the inspired air) with respect to the baseline (expressed as a percentage of changes from the baseline, e.g. % Δf_R). The magnitude of the % Δf_R, % ΔV_T, and % ΔV_E were not different in female and male during hypoxia, therefore we combined all the data from both sexes. Overall, changing the inspired O_2 from 21% (room air) to 10% did not elicit ventilatory response in adult marmosets (Figure 5). However, during hypoxia, the metabolic rate (MR) was decreased by ~ 35%.

Hypercapnic Ventilatory Response

We then measured changes in f_R, V_T, and V_E before and during hypercapnic challenge (6% CO_2 in the inspired air). Similar to hypoxia, the magnitude of the % Δf_R, % ΔV_T, and % ΔV_E in female and male during systemic hypercapnia were similar. Increasing CO_2 inside the chamber augmented frequency (% Δf_R, by 40 ± 4%), V_T (by 191 ± 20%), and V_E (by 306 ± 22%; Figure 6).

Regularity of breathing

The cycle-to-cycle dispersion of T_{TOT} in female and male marmosets were shown in Poincaré plots (Figure 7). We also quantified the regularity of breathing (9) by SD1 and SD2 (see Methods and (19)). The baseline SD1 was similar between female and male marmosets (608 ± 165 vs. 490 ± 185 respectively, Figure 7). The baseline SD2 was also comparable in female *vs.* male marmosets (846 ± 253 *vs.* 619 ± 222, respectively, Figure 7).

Sigh frequency, sniffing, and apnea index

Since incidences of sighs, apneas, and sniffing could contribute to the irregularity of respiration, we measured frequencies of these essential features of breathing behavior. It has been shown that sigh can be generated within the inspiratory rhythm-generating circuits of the preBötC (6,20–24), and may be modulated by excitatory signals from central chemocenters (6,9,20,25,26). In adult marmosets, sigh frequencies were not different when compared to those in male animals during the baseline (12 ± 2 vs. 12 ± 3 hr^{-1} in

male). It has also been shown that hypoxia increases frequency of sighs in rodents (6,20). Consistent with those results, hypoxia increased sigh events by average of 3.5-folds (12 ± 2 vs. 36 ± 10 hr^{-1} in room air; Figure 8).

Spontaneous and post-sigh apneas are reported in the rodents, rabbits, humans, and other animals (9,27–32). On average, marmosets at room air showed 29 ± 19 hr^{-1} spontaneous apneas, and we did not find differences in apnea index between female and male marmosets.

Lastly, we analyzed high frequency breathing (sniffing) in marmosets. On average, marmosets spent 139 ± 46 sec hr^{-1} sniffing during the baseline recording and there were no differences in sniffing time between female and male marmosets (133 ± 110 vs. 144 ± 39 sec hr^{-1} in male). Neither hypoxia nor hypercapnia changed the sniffing time (data not shown).

Discussions

We used non-invasive, Whole-body Plethysmography to measure breathing behaviors (6,33) in unrestrained, freely moving, awake marmosets. Plethysmography has a simple and robust design that has been used widely in humans [neonates (34) and adults (35)], non-human primates [such as macaques (36) and cynomolgus monkeys (13)], rodents (6,33), dogs (37), sheep (38), cats (39), turtles (40), and other animals.

The common marmoset (*Callithrix jacchus*) is a small New World primate (41). Recently marmosets have been proposed as a powerful animal model in neuroscience research (42–45), especially to study vocal communication (46). Compared to rodents, marmoset's central nervous system more closely resemble humans' in terms of physiological function and anatomy of the brain (47). It was proposed recently that using marmosets in physiological research can fill the gap between rodents' and humans' studies (11). In addition, considering the similarity of the brain structure and circuit connectivity between primates, marmosets provide an attractive opportunity to study cortical (i.e., voluntary) control of respiratory motor activity (48) as well as coordination of complex respiratory functions during vocalization. Accordingly, in this study, we used Whole-body Plethysmography to characterize respiratory behaviors in awake, freely behaving adult marmosets.

Using the whole-body respiratory measurement in conscious animals requires sophisticated algorithms to distinguish the respiratory signals from noises (i.e., movements). To avoid this problem, respiratory activities are often recorded when the animal is asleep or anesthetized. There are absolute advantages to studying the homeostatic control of breathing physiology in awake animals, despite the increased variability. Therefore, to overcome this challenging task, we validated and used a new Python package, Neurokit2 (see Methods section), for unsupervised analysis of respiratory signals obtained from experimental animals. We then tested the ventilatory response to hypercapnia (increased inspired CO_2 to 6%). Currently, it has been postulated that distributed chemosensitive regions in the rodent's medulla (49–53) act as central respiratory chemosensors and are responsible for mounting of about 70% of the hypercapnic respiratory response (the mechanism that adjusts breathing in accordance with increase in PCO_2). Specialized peripheral chemoreceptors located in the carotid bodies (and aortic bodies in some species) are responsible to the remaining 30% of hypercapnia-induced augmentation of breathing.

In our experiments, to minimize the input from peripheral chemosensors, we applied hyperoxic hypercapnia (60% O_2/6% CO_2 balanced with N_2) as it has been shown that hyperoxia (> 50% O_2 in inspired air) inhibit the drive from the carotid body chemoreceptors (54,55). Since marmosets lack aortic bodies (56), the hypercapnic ventilatory response reported here is driven by the central CO_2 respiratory chemocenters. It is proposed that neurons and astrocytes in the retrotrapezoid nucleus (RTN), medullary raphé, and preBötC are primarily responsible for central CO_2 sensing in rodents (6,57–61). Recently the RTN was mapped in rhesus macaque's brainstem, a species of Old-World monkeys (62), however, the location of RTN, raphé, preBötC, and other respiratory centers have not yet been mapped in marmosets.

In awake, freely behaving marmosets, hyperoxic hypercapnia increased both f_R and V_T (Figure 6). However, the augmentation of ventilation (V_E) was mainly due to increase in V_T (by ~ 250%) rather than f_R. These preliminary data are comparable to data from human (63) as well as recent data obtained from conscious rodents (11,64).

The hypoxic ventilatory response (HVR) in common marmoset was absolutely interesting as there was little or no increase in f_R and V_T during hypoxic exposure (Figure 6). Other than HVR, mammals can reduce oxygen demand by optimizing and decreasing the rate of their metabolism (65). During hypoxia, adult marmosets, decreased their metabolic rates by ~ 35%, which is consistent with previous data from cats (66), rodents (67), pygmy marmosets (68) and human (69,70).

Although hypoxic conditions (low inspired O_2) in marmoset's habitat (sea-level forests of the Amazon) are rare, hypoxia might occur during sleep (i.e., sleep apnea) or as a result of a disease state. It is commonly believed that the HVR is biphasic in adult mammals. During acute hypoxia, ventilation is depicted by an initial increase followed by a subsequent decline to a value above the baseline. This biphasic hypoxic response has been reported in humans, rats, and other mammals (71–75). It is believed that the rapid initial hypoxic-induced increase in V_E is due to activation of peripheral chemosensors (i.e., carotid bodies). The mechanism of hypoxic ventilatory decline (HVD) is not fully understood. It is proposed that desensitization of peripheral chemoreceptors might have a role (76), though significant evidence suggest that, at least in rodents, astrocytes (the numerous star-shaped glia cells) in preBötC (6,8,77) and RTN (78,79) are capable of acting as central respiratory oxygen chemosensors and contribute to the HVD possibly via vesicular release of adenosine triphosphate (ATP). In addition to preBötC and RTN, rostral ventrolateral medulla (rVLM) and the nucleus of the solitary tract (NTS) in the brainstem are proposed to have oxygen sensing capabilities (80,81). However, more research is required to understand if the 'distributed central oxygen chemosensors' hypothesis (11) can be generalized to primates.

The brain is highly susceptible to low oxygen levels. Supply of oxygen may be decreased in clinical conditions (such as sleep apnea or stroke) or environmental settings (such as exposure to carbon monoxide). Therefore, an understanding of how the brain maintains homeostatic levels of oxygen and responds to hypoxic events is of longstanding interest. Studies in common marmosets will shed some light on this problem and might fill the gap between rodent and human research to better understand the homeostatic control of breathing and its disorders.

References

1. Smith JC, Ellenberger HH, Ballanyi K, Richter DW, Feldman JL. Pre-Bötzinger complex: a brainstem region that may generate respiratory rhythm in mammals. Science. 1991 Nov 1;254(5032):726–9.
2. Del Negro CA, Funk GD, Feldman JL. Breathing matters. Nat Rev Neurosci. 2018;19(6):351–67.
3. Heymans C, Bouckaert JJ. Sinus caroticus and respiratory reflexes. J Physiol (Lond). 1930 Apr 14;69(2):254–66.
4. O'Regan RG, Majcherczyk S. Role of peripheral chemoreceptors and central chemosensitivity in the regulation of respiration and circulation. J Exp Biol. 1982 Oct;100:23–40.
5. Guyenet PG. Regulation of breathing and autonomic outflows by chemoreceptors. Compr Physiol. 2014 Oct;4(4):1511–62.
6. Sheikhbahaei S, Turovsky EA, Hosford PS, Hadjihambi A, Theparambil SM, Liu B, et al. Astrocytes modulate brainstem respiratory rhythm-generating circuits and determine exercise capacity. Nat Commun. 2018 Jan 25;9(1):370.
7. Sheikhbahaei S, Smith JC. Breathing to inspire and arouse. Science. 2017 Mar 31;355(6332):1370–1.
8. Angelova PR, Kasymov V, Christie I, Sheikhbahaei S, Turovsky E, Marina N, et al. Functional oxygen sensitivity of astrocytes. J Neurosci. 2015 Jul 22;35(29):10460–73.
9. Sheikhbahaei S, Gourine AV, Smith JC. Respiratory rhythm irregularity after carotid body denervation in rats. Respir Physiol Neurobiol. 2017 Aug 4;246:92–7.
10. Hazari MS, Farraj AK. Comparative control of respiration. Comparative biology of the normal lung. Elsevier; 2015. p. 245–88.
11. Sheikhbahaei S. Physiology: New Insights Into Central Oxygen Sensing. Curr Biol. 2020;
12. Abbott DH, Barnett DK, Colman RJ, Yamamoto ME, Schultz-Darken NJ. Aspects of common marmoset basic biology and life history important for biomedical research. Comp Med. 2003 Aug;53(4):339–50.
13. Iizuka H, Sasaki K, Odagiri N, Obo M, Imaizumi M, Atai H. Measurement of respiratory function using whole-body plethysmography in unanesthetized and unrestrained nonhuman primates. J Toxicol Sci. 2010 Dec;35(6):863–70.
14. Van Rossum G, Drake FL. The python language reference manual. 2011;
15. Garcia S, Guarino D, Jaillet F, Jennings T, Pröpper R, Rautenberg PL, et al. Neo: an object model for handling electrophysiology data in multiple formats. Front Neuroinformatics. 2014 Feb 20;8:10.
16. McKinney W. Data structures for statistical computing in python. Proceedings of the 9th Python in Science. 2010;
17. van der Walt S, Colbert SC, Varoquaux G. The NumPy Array: A Structure for Efficient Numerical Computation. Comput Sci Eng. 2011 Mar;13(2):22–30.
18. Makowski D, Pham T, Zen J, Brammer JC, Le D, Hung Pham (Phạm Tiến Hùng), et al. NeuroKit2: A Python Toolbox for Neurophysiological Signal Processing. Zenodo. 2020;
19. Soni R, Muniyandi M. Breath rate variability: A novel measure to study the meditation effects. Int J Yoga. 2019 Apr;12(1):45–54.
20. Li P, Janczewski WA, Yackle K, Kam K, Pagliardini S, Krasnow MA, et al. The peptidergic control circuit for sighing. Nature. 2016 Feb 18;530(7590):293–7.
21. Lieske SP, Thoby-Brisson M, Telgkamp P, Ramirez JM. Reconfiguration of the neural

network controlling multiple breathing patterns: eupnea, sighs and gasps. Nat Neurosci. 2000;
22. Borrus DS, Grover C, Conradi Smith GD, Del Negro CA. Role of synaptic inhibition in the coupling of the respiratory rhythms that underlie eupnea and sigh behaviors. Eneuro. 2020 May 11;
23. Toporikova N, Chevalier M, Thoby-Brisson M. Sigh and eupnea rhythmogenesis involve distinct interconnected subpopulations: A combined computational and experimental study. Eneuro. 2015 Apr 22;2(2).
24. Vlemincx E, Abelson JL, Lehrer PM, Davenport PW, Van Diest I, Van den Bergh O. Respiratory variability and sighing: a psychophysiological reset model. Biol Psychol. 2013 Apr;93(1):24–32.
25. Souza GMPR, Kanbar R, Stornetta DS, Abbott SBG, Stornetta RL, Guyenet PG. Breathing regulation and blood gas homeostasis after near complete lesions of the retrotrapezoid nucleus in adult rats. J Physiol (Lond). 2018 Jul;596(13):2521–45.
26. Souza GMPR, Stornetta RL, Stornetta DS, Abbott SBG, Guyenet PG. Contribution of the retrotrapezoid nucleus and carotid bodies to arousal from sleep elicited by hypercapnia and hypoxia. J Neurosci. 2019 Oct 21;
27. Yamauchi M, Ocak H, Dostal J, Jacono FJ, Loparo KA, Strohl KP. Post-sigh breathing behavior and spontaneous pauses in the C57BL/6J (B6) mouse. Respir Physiol Neurobiol. 2008 Jul 31;162(2):117–25.
28. Franco P, Verheulpen D, Valente F, Kelmanson I, de Broca A, Scaillet S, et al. Autonomic responses to sighs in healthy infants and in victims of sudden infant death. Sleep Med. 2003 Nov;4(6):569–77.
29. van der Heijden ME, Zoghbi HY. Loss of Atoh1 from neurons regulating hypoxic and hypercapnic chemoresponses causes neonatal respiratory failure in mice. Elife. 2018 Jul 4;7.
30. Bongianni F, Mutolo D, Cinelli E, Pantaleo T. Respiratory responses induced by blockades of GABA and glycine receptors within the Bötzinger complex and the pre-Bötzinger complex of the rabbit. Brain Res. 2010 Jul 16;1344:134–47.
31. Li Y, Song G, Cao Y, Wang H, Wang G, Yu S, et al. Modulation of the Hering-Breuer reflex by raphe pallidus in rabbits. Neurosci Lett. 2006 Apr 24;397(3):259–62.
32. Ramirez J-M, Garcia AJ, Anderson TM, Koschnitzky JE, Peng Y-J, Kumar GK, et al. Central and peripheral factors contributing to obstructive sleep apneas. Respir Physiol Neurobiol. 2013 Nov 1;189(2):344–53.
33. Hamelmann E, Schwarze J, Takeda K, Oshiba A, Larsen GL, Irvin CG, et al. Noninvasive measurement of airway responsiveness in allergic mice using barometric plethysmography. Am J Respir Crit Care Med. 1997 Sep;156(3 Pt 1):766–75.
34. Sivieri EM, Dysart K, Abbasi S. Evaluation of pulmonary function in the neonate. Fetal and neonatal physiology. Elsevier; 2017. p. 754–765.e3.
35. Dubois AB, Botelho SY, Bedell GN, Marshall R, Comroe JH. A rapid plethysmographic method for measuring thoracic gas volume: a comparison with a nitrogen washout method for measuring functional residual capacity in normal subjects. J Clin Invest. 1956 Mar;35(3):322–6.
36. Besch TK, Ruble DL, Gibbs PH, Pitt ML. Steady-state minute volume determination by body-only plethysmography in juvenile rhesus monkeys. Lab Anim Sci. 1996 Oct;46(5):539–44.

37. Liu NC, Adams VJ, Kalmar L, Ladlow JF, Sargan DR. Whole-Body Barometric Plethysmography Characterizes Upper Airway Obstruction in 3 Brachycephalic Breeds of Dogs. J Vet Intern Med. 2016 May 9;30(3):853–65.
38. Hutchison AA, Hinson JM, Brigham KL, Snapper JR. Effect of endotoxin on airway responsiveness to aerosol histamine in sheep. J Appl Physiol. 1983 Jun;54(6):1463–8.
39. Hoffman AM, Dhupa N, Cimetti L. Airway reactivity measured by barometric whole-body plethysmography in healthy cats. Am J Vet Res. 1999 Dec;60(12):1487–92.
40. Valente ALS, Martínez-Silvestre A, García-Guasch L, Riera-Tort A, Marco I, Lavin S, et al. Evaluation of pulmonary function in European land tortoises using whole-body plethysmography. Vet Rec. 2012 Aug 11;171(6):154, 1–5.
41. Okano H, Miyawaki A, Kasai K. Brain/MINDS: brain-mapping project in Japan. Philos Trans R Soc Lond B, Biol Sci. 2015 May 19;370(1668).
42. Miller CT, Freiwald WA, Leopold DA, Mitchell JF, Silva AC, Wang X. Marmosets: A neuroscientific model of human social behavior. Neuron. 2016 Apr 20;90(2):219–33.
43. Burkart JM, Finkenwirth C. Marmosets as model species in neuroscience and evolutionary anthropology. Neurosci Res. 2015 Apr;93:8–19.
44. Leopold DA, Mitchell JF, Freiwald WA. Evolved Mechanisms of High-Level Visual Perception in Primates. Evolution of nervous systems. Elsevier; 2017. p. 203–35.
45. Mitchell JF, Leopold DA. The marmoset monkey as a model for visual neuroscience. Neurosci Res. 2015 Apr;93:20–46.
46. Eliades SJ, Miller CT. Marmoset vocal communication: Behavior and neurobiology. Dev Neurobiol. 2017;77(3):286–99.
47. Bendor D, Wang X. The neuronal representation of pitch in primate auditory cortex. Nature. 2005 Aug 25;436(7054):1161–5.
48. Walker J, MacLean J, Hatsopoulos NG. The marmoset as a model system for studying voluntary motor control. Dev Neurobiol. 2017 Mar;77(3):273–85.
49. Nattie E. CO2, brainstem chemoreceptors and breathing. Prog Neurobiol. 1999 Nov;59(4):299–331.
50. Nattie E. Multiple sites for central chemoreception: their roles in response sensitivity and in sleep and wakefulness. Respir Physiol. 2000 Sep;122(2–3):223–35.
51. Nattie EE. Central chemosensitivity, sleep, and wakefulness. Respir Physiol. 2001 Dec;129(1–2):257–68.
52. Spyer KM, Thomas T. Sensing arterial CO(2) levels: a role for medullary P2X receptors. J Auton Nerv Syst. 2000 Jul 3;81(1–3):228–35.
53. Nattie E, Li A. Central chemoreception is a complex system function that involves multiple brain stem sites. J Appl Physiol. 2009 Apr;106(4):1464–6.
54. Chavez-Valdez R, Mason A, Nunes AR, Northington FJ, Tankersley C, Ahlawat R, et al. Effect of hyperoxic exposure during early development on neurotrophin expression in the carotid body and nucleus tractus solitarii. J Appl Physiol. 2012 May;112(10):1762–72.
55. Gonzalez C, Almaraz L, Obeso A, Rigual R. Carotid body chemoreceptors: from natural stimuli to sensory discharges. Physiol Rev. 1994 Oct;74(4):829–98.
56. Clarke JA, de B Daly M. The distribution of presumptive thoracic paraganglionic tissue in the common marmoset (Callithrix jacchus). Braz J Med Biol Res. 2002 Apr;35(4):437–44.
57. Kumar NN, Velic A, Soliz J, Shi Y, Li K, Wang S, et al. Regulation of breathing by CO_2 requires the proton-activated receptor GPR4 in retrotrapezoid nucleus neurons. Science. 2015 Jun 12;348(6240):1255–60.

58. Teran FA, Massey CA, Richerson GB. Serotonin neurons and central respiratory chemoreception: where are we now? Prog Brain Res. 2014;209:207–33.
59. Solomon IC, Edelman NH, O'Neal MH. CO(2)/H(+) chemoreception in the cat pre-Bötzinger complex in vivo. J Appl Physiol. 2000 Jun;88(6):1996–2007.
60. Gourine AV, Kasymov V, Marina N, Tang F, Figueiredo MF, Lane S, et al. Astrocytes control breathing through pH-dependent release of ATP. Science. 2010 Jul 30;329(5991):571–5.
61. Koizumi H, Smerin SE, Yamanishi T, Moorjani BR, Zhang R, Smith JC. TASK channels contribute to the K+-dominated leak current regulating respiratory rhythm generation in vitro. J Neurosci. 2010 Mar 24;30(12):4273–84.
62. Levy J, Facchinetti P, Jan C, Achour M, Bouvier C, Brunet J-F, et al. Tridimensional mapping of Phox2b expressing neurons in the brainstem of adult Macaca fascicularis and identification of the retrotrapezoid nucleus. J Comp Neurol. 2019 Dec 1;527(17):2875–84.
63. Duffin J, Mohan RM, Vasiliou P, Stephenson R, Mahamed S. A model of the chemoreflex control of breathing in humans: model parameters measurement. Respir Physiol. 2000 Mar;120(1):13–26.
64. Bhandare A, van de Wiel J, Roberts R, Braren I, Huckstepp R, Dale N. Analyzing the neuroglial brainstem circuits for respiratory chemosensitivity in freely moving mice. BioRxiv. 2020 May 11;
65. Dzal YA, Jenkin SEM, Lague SL, Reichert MN, York JM, Pamenter ME. Oxygen in demand: How oxygen has shaped vertebrate physiology. Comp Biochem Physiol Part A, Mol Integr Physiol. 2015 Aug;186:4–26.
66. Gautier H, Bonora M, Remmers JE. Effects of hypoxia on metabolic rate of conscious adult cats during cold exposure. J Appl Physiol. 1989 Jul;67(1):32–8.
67. Mortola JP, Matsuoka T, Saiki C, Naso L. Metabolism and ventilation in hypoxic rats: effect of body mass. Respir Physiol. 1994 Jul;97(2):225–34.
68. Tattersall GJ, Blank JL, Wood SC. Ventilatory and metabolic responses to hypoxia in the smallest simian primate, the pygmy marmoset. J Appl Physiol. 2002 Jan;92(1):202–10.
69. Murray AJ. Energy metabolism and the high-altitude environment. Exp Physiol. 2016 Jan;101(1):23–7.
70. Robinson KA, Haymes EM. Metabolic effects of exposure to hypoxia plus cold at rest and during exercise in humans. J Appl Physiol. 1990 Feb;68(2):720–5.
71. Eden GJ, Hanson MA. Maturation of the respiratory response to acute hypoxia in the newborn rat. J Physiol (Lond). 1987 Nov;392:1–9.
72. Martin RJ, van Lunteren E, Haxhiu MA, Carlo WA. Upper airway muscle and diaphragm responses to hypoxia in the piglet. J Appl Physiol. 1990 Feb;68(2):672–7.
73. Fung ML, Wang W, Darnall RA, St John WM. Characterization of ventilatory responses to hypoxia in neonatal rats. Respir Physiol. 1996 Jan;103(1):57–66.
74. Dahan A, Ward D, van den Elsen M, Temp J, Berkenbosch A. Influence of reduced carotid body drive during sustained hypoxia on hypoxic depression of ventilation in humans. J Appl Physiol. 1996 Aug;81(2):565–72.
75. Vizek M, Bonora M. Diaphragmatic activity during biphasic ventilatory response to hypoxia in rats. Respir Physiol. 1998 Feb;111(2):153–62.
76. Bascom DA, Clement ID, Cunningham DA, Painter R, Robbins PA. Changes in peripheral chemoreflex sensitivity during sustained, isocapnic hypoxia. Respir Physiol. 1990 Nov;82(2):161–76.

77. Rajani V, Zhang Y, Jalubula V, Rancic V, SheikhBahaei S, Zwicker JD, et al. Release of ATP by pre-Bötzinger complex astrocytes contributes to the hypoxic ventilatory response via a Ca^{2+} -dependent $P2Y_1$ receptor mechanism. J Physiol. 2018 Aug;596(15):3245–69.
78. Uchiyama M, Nakao A, Kurita Y, Fukushi I, Takeda K, Numata T, et al. O2-Dependent Protein Internalization Underlies Astrocytic Sensing of Acute Hypoxia by Restricting Multimodal TRPA1 Channel Responses. Curr Biol. 2020 Jul 9;
79. Czeisler CM, Silva TM, Fair SR, Liu J, Tupal S, Kaya B, et al. The role of PHOX2B-derived astrocytes in chemosensory control of breathing and sleep homeostasis. J Physiol (Lond). 2019 Mar 19;597(8):2225–51.
80. Accorsi-Mendonça D, Almado CEL, Bonagamba LGH, Castania JA, Moraes DJA, Machado BH. Enhanced Firing in NTS Induced by Short-Term Sustained Hypoxia Is Modulated by Glia-Neuron Interaction. J Neurosci. 2015 Apr 29;35(17):6903–17.
81. Mazza E, Edelman NH, Neubauer JA. Hypoxic excitation in neurons cultured from the rostral ventrolateral medulla of the neonatal rat. J Appl Physiol. 2000 Jun;88(6):2319–29.

Figure 1

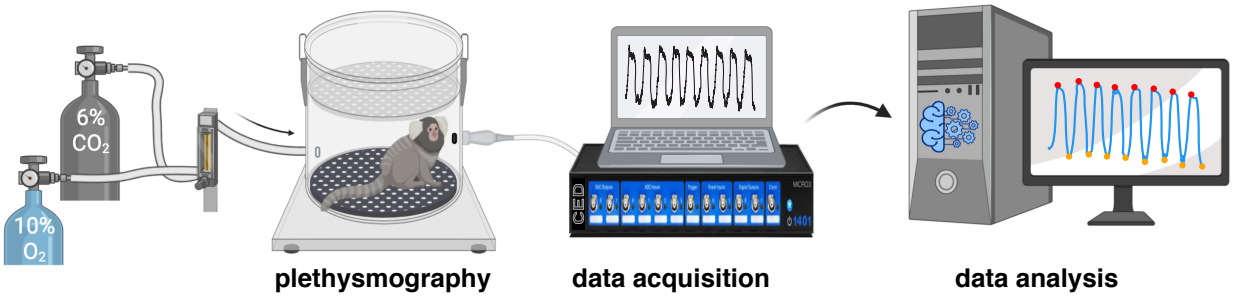

Figure 1 | Experimental pipeline for measurement and analysis of marmoset respiratory behaviors. After a 40-minute baseline period at room air (21% O_2), the breathing behavior of animal was studied under either hypoxic (10% O_2; 10 min) or hypercapnic (6% CO_2; 10 min) conditions. Raw respiratory signal is later cleaned and analyzed offline (see Methods for details).

Figure 2

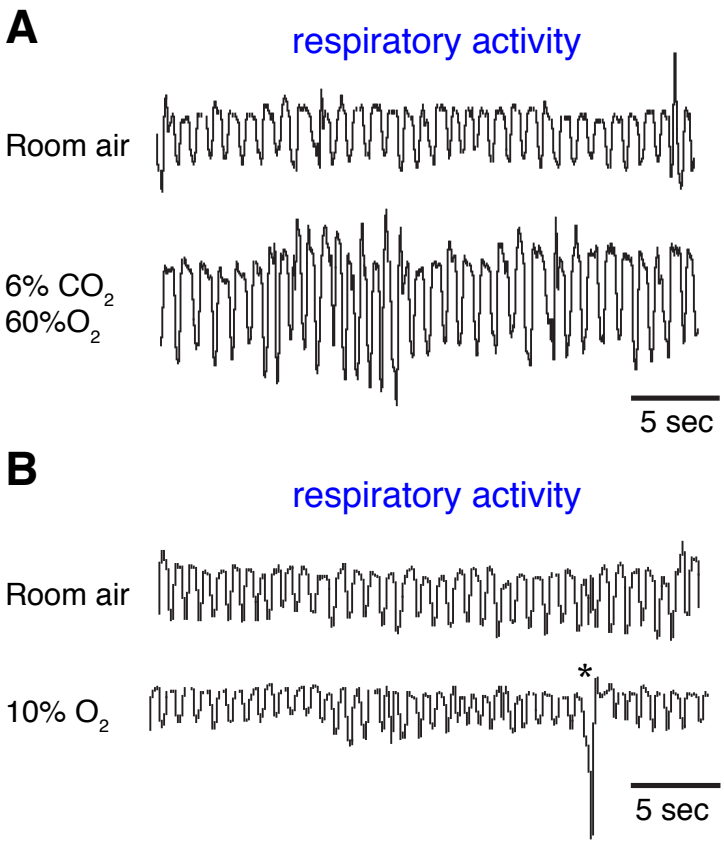

Figure 2 | Breathing behaviors in adult marmoset. Representative raw respiratory traces at baseline and following 5 min exposure to hypoxic (**A**) and 5 min exposure to hypercapnic (**B**) conditions. * represent a sigh breathing.

Figure 3

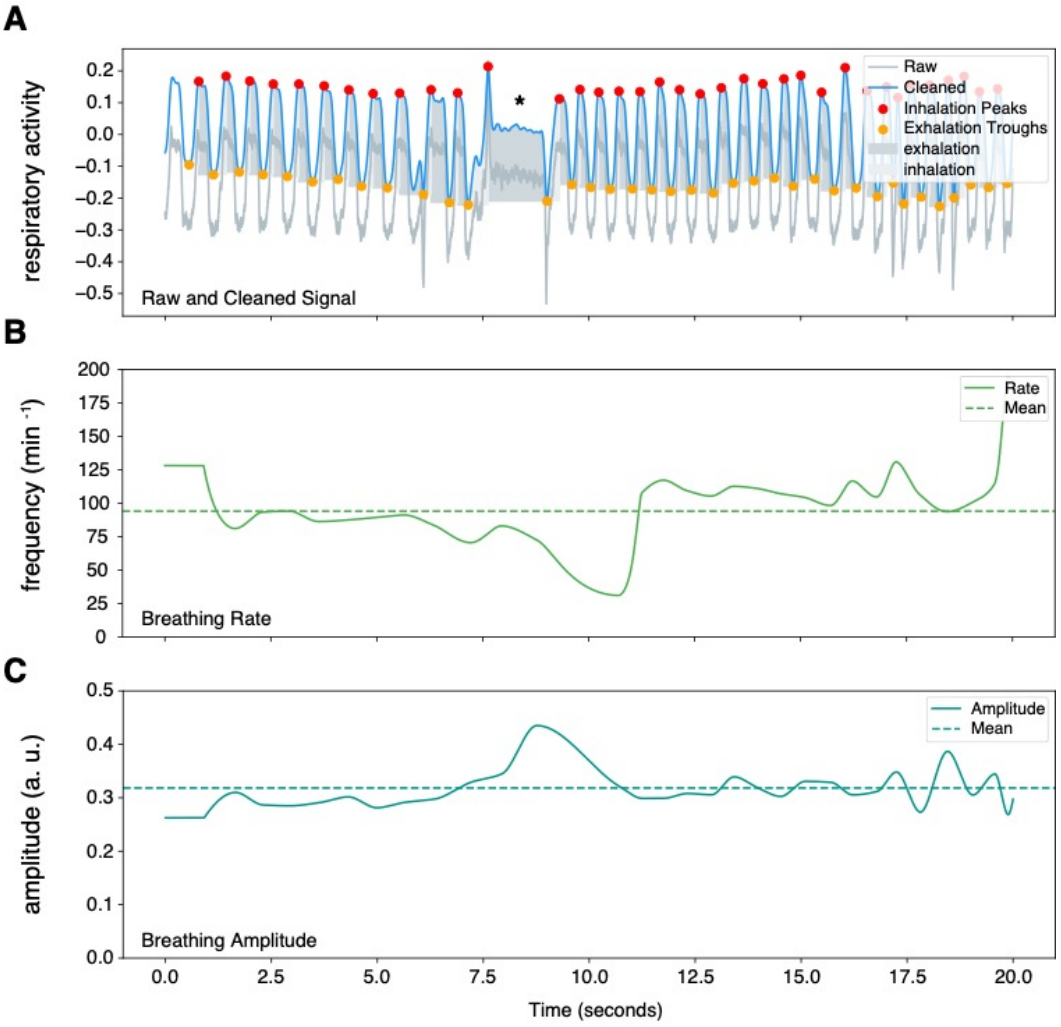

Figure 3 | Sample plot output from NeuroKit2 Python package. Respiratory trace is sampled from a single male marmoset during hypercapnia challenge. (**A**) NeuroKit2 was used for signal detrending and smoothing, peak and trough extraction, as well as respiratory phase. (**B & C**) We also used NeuroKit2 methods for instantaneous measurement of breathing rate (**B**) and breathing amplitude (**C**). * represents respiratory changes during a phee call.

Figure 4

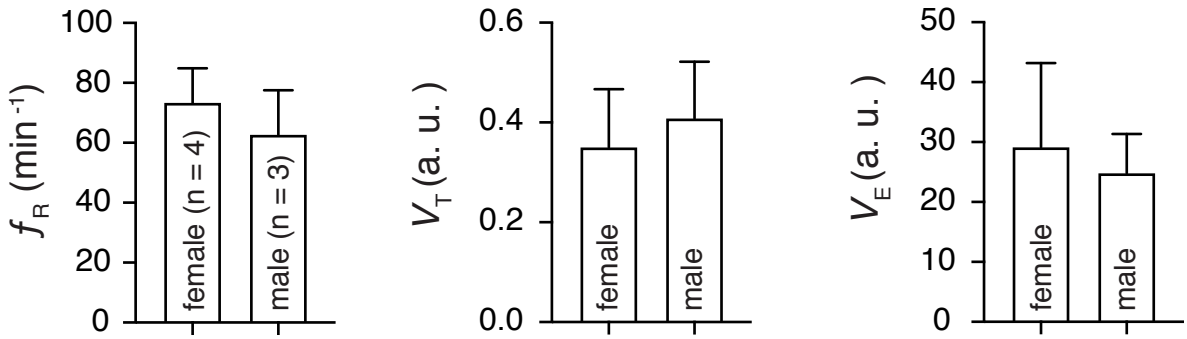

Figure 4 | Sex differences in baseline respiratory frequencies. Baseline respiratory frequencies (f_R), tidal volumes (V_T), and minute ventilations (V_E) were not different between female (n = 4) and male (n = 3) marmosets. Data are shown as mean rate ± SEM. a. u. – arbitrary unit.

Figure 5

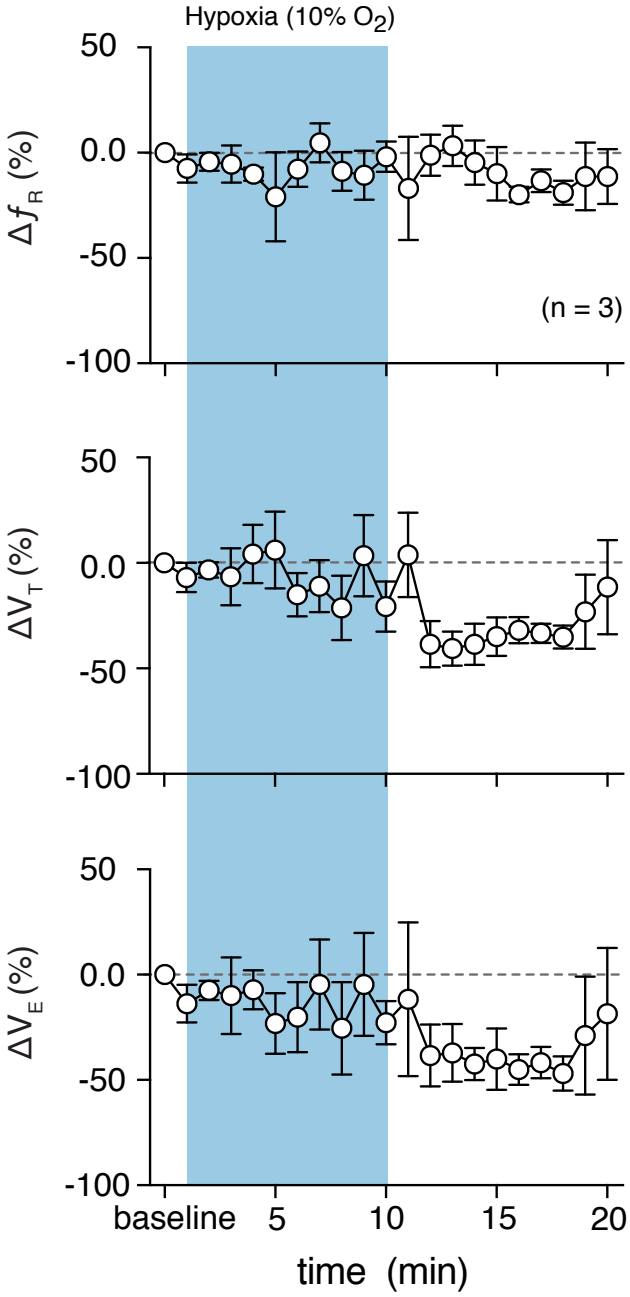

Figure 5 | Hypoxic challenge induced changes in respiratory behavior. Measurements of breathing rate (f_R), tidal volume (V_T), and minute ventilation (V_E) were averaged across 1-minute epochs for assessment of local changes in each parameter. Data are shown as mean percent change from baseline ± SEM. During a 10-minute hypoxia challenge we saw no changes in f_R, V_T, and V_E compared to baseline.

Figure 6

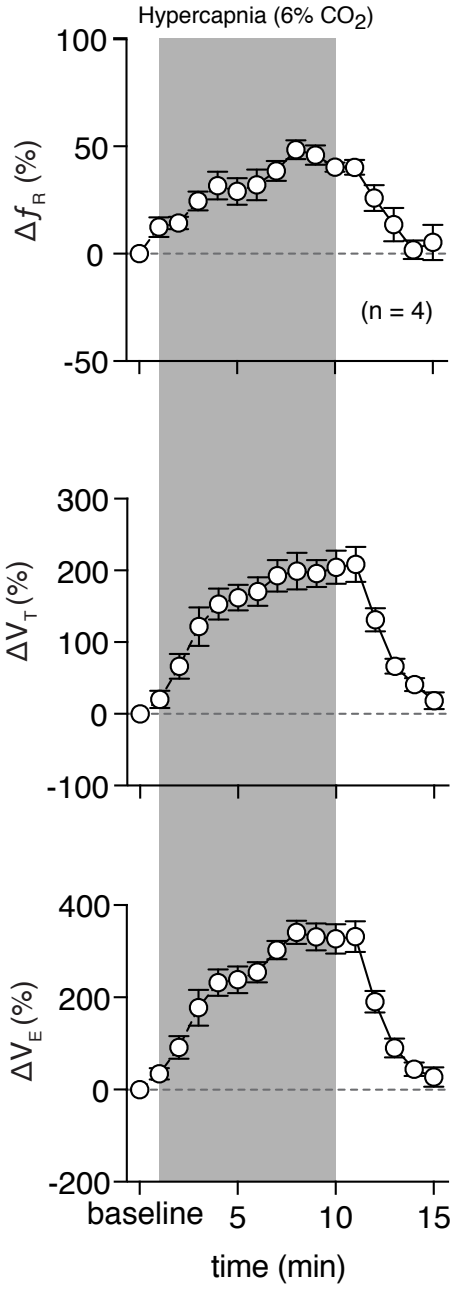

Figure 6 | Hypercapnia challenge induced changes in respiratory behavior. Measurements of breathing rate (f_R), tidal volume (V_T), and minute ventilation (V_E) were averaged across 1-minute epochs for assessment of local changes in each parameter. Data are shown as mean percent change from baseline ± SEM.

Figure 7

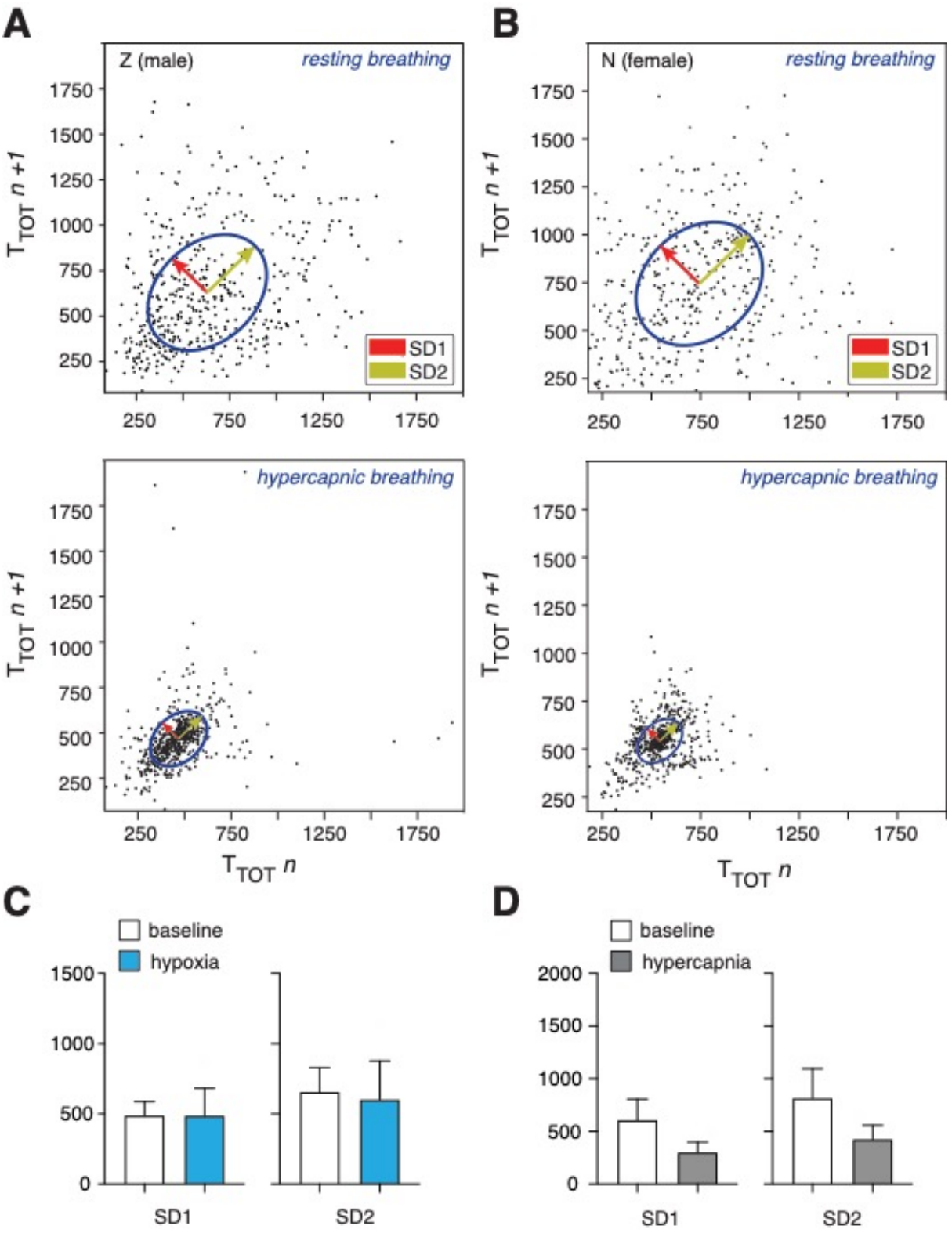

Figure 7 | Changes in respiratory rate variability following hypoxia and hypercapnia challenge. Representative Poincaré plots of total cycle duration (T_{TOT}) for nth cycle versus T_{TOT} for n+1 cycle during baseline and hypercapnic air conditions in male (**A**) and female (**B**) marmosets. (**C**) Summary data of changes in SD1 and SD2 during hypoxia challenge. Neither measure of respiratory rate variability was different from baseline following the hypoxia challenge. (**D**) Summary data of changes in SD1 and SD2 during hypercapnia challenge. Respiratory rate variability decreased during the challenge across both measures. Data are shown as mean ± SEM.

Figure 8

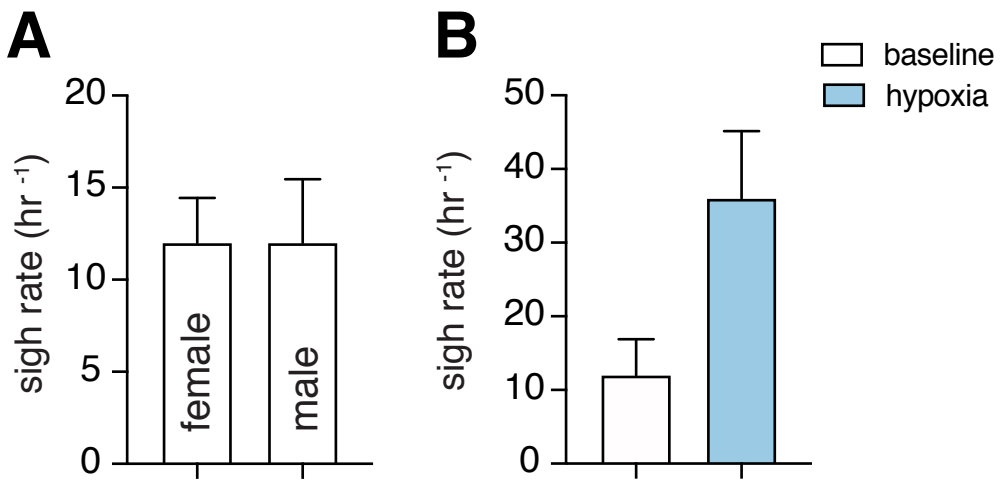

Figure 8 | Sigh frequencies between sexes and following hypoxia challenge. (**A**) Sigh frequency at baseline air was not different between sexes (n = 3 males, n = 4 females). (**B**) Summary data illustrating increase in sigh frequency during hypoxic condition (10% O_2). Data are shown as mean ± SEM.